GaN lateral PolarSJs: polarization-doped super junctions

Bo Song*, Mingda Zhu, Zongyang Hu, Erhard Kohn, Debdeep Jena and Huili (Grace) Xing*
Department of Electrical Engineering, University of Notre Dame, Notre Dame, IN 46556, USA
*Email: bsong@nd.edu and hxing@nd.edu

Background: Wide bandgap semiconductors (WBG) offer the most compelling solutions for power electronics owing to their large breakdown electric field (E_b) and high carrier mobilities. The Baliga's figure of merit ($\varepsilon\mu E_b^3$) of WBGs including GaN and SiC is ~100X higher than that of Si. On the other hand, super junction (SJ) diodes can break the limitation of the trade-off relationship between area specific-on resistance ($R_{on,sp}$) and breakdown voltage (BV) in conventional p-n junctions [1-2]. The combination of the super junction technology and GaN material would further boost the performance. Indeed, simulation results on GaN super junctions have shown great performance enhancement, but no practical solution for fabrication such device has been proposed and the challenge remains unsolved [3]. GaN natural super junction (NSJ) has been proposed and realized [4], but the high carrier densities of 2DEG and 2DHG layers result in severe electrical field crowding (similar to the field crowding near the gate on the drain side in HEMT) and the performances are far below expectation. An innovative technology to realize GaN super junction devices is highly desirable.

Proposed Device: Here we propose a lateral polarization-doped super junction (LPSJ) shown in Fig.1 (b): the n/p pillar regions are realized by compositionally grading AlGaN, and the n^+ and p^+ cathode/anode regions are formed by regrowth to connect with the n and p pillars, respectively. First, it is important to note that the high spontaneous and piezoelectric polarization charges in the GaN family are absent in Si and SiC. This unique feature is the key enabler for the proposed LPSJ. Second, both n and p type polarization doping as well as n^+ and p^+ regrowth has been demonstrated by our group [5-8]. More recently, polarization-doped p-n junctions have been also demonstrated by several groups including our own [9-10]. To realize the super junction, i.e. n/p pillars with balanced charges, one only needs to linearly grade from GaN to Al_xGaN and then grading back to GaN during epitaxial growth, without any ion implantation process. The doping profile of the pillars can be precisely controlled by MBE/MOCVD growth in terms of Al composition and layer thickness, thus suppressing the charge imbalance problem. Since the charges are spread over the graded layers, the field crowding effect due to the high carrier densities in NSJ can be avoided.

Analytical Relationship between BV and $R_{on,sp}$: Starting from $R_{on,sp_L} = \frac{1}{q\mu N_D} \times \frac{L_{drift}}{wh'} \times A = \frac{1}{q\mu N_D} \times \frac{L_{drift}}{wh'} \times wL_{drift}$, $R_{on,sp}$ of the LPSJ can be expressed as $R_{on,sp_L} = \frac{BV^2}{q\sigma_\pi \bar{\mu} E_c^2} \times \frac{2d^2}{h(d-d_{dep})}$ where $\bar{\mu}$ is the average mobility for the grading layer. The detailed derivation is shown in the next page. Since the carrier mobility is Al composition dependent, it varies along the vertical direction. An average mobility has been used to calculate $R_{on,sp}$ for the lateral current flow. For conventional GaN lateral p-n diodes, $R_{on,sp}$ can be expressed as $R_{on,sp_L} = \frac{8}{\varepsilon_s \mu h} \times \frac{BV^3}{E_c^4}$.

Results and discussion: First, low field mobility in the drift region has been modeled; shown in Fig. 2(a) and Fig. 2(b) are the electron mobility in Si-doped GaN and that in polarization-doped AlGaN layers [11]. The average mobility in the graded AlGaN n-pillars can be thus obtained by $\frac{1}{\bar{\mu}} = \frac{\int \frac{n(y)}{\mu(y)} dy}{\int n(y) dy}$. E.g. in a linearly graded Al_xGaN with x_{Al} =0→ 10%, an average electron mobility of 1073 cm^2/Vs is obtained; for a pillar thickness of 560 nm, the polarization doping concentration is ~2e16 cm^{-3}. In comparison, the mobility in Si-doped GaN is ~1000-1600 cm^2/Vs for n~$1x10^{16}$-$1x10^{17}$ cm^{-3}. The ideal specific on-resistance and breakdown voltage between the conventional p-n junction and the LPSJ with linearly graded Al_xGaN pillars (x_{Al} = 0→30%) are compared in Fig. 2(c), where the total height h of 4 μm and a critical electric field E_C of 3.6 MV/cm are used. It is observed that for BV > 300 V, the LPSJ offers significantly lower $R_{on,sp}$; for instance, a >10x reduction in $R_{on,sp}$ is predicted around 1200 V and a >100x reduction in $R_{on,sp}$ for 10 kV. Fig.2 (d) shows the $R_{on,sp}$ as a function of the pillar width d, where in general a smaller pillar width results in a lower $R_{on,sp}$. This is expected since for the same compositional grading range, a small pillar width leads to a high carrier concentration, thus a low $R_{on,sp}$. An optimized pillar width of ~ 200 nm is found for linearly graded Al_xGaN pillars with x_{Al} =0→ 20%, which is mainly attributed to the fact that the total depletion width in the n-region becomes comparable with or smaller than the pillar size for d < 200 nm. The field crowding in the NSJ and the LPSJ is compared in Fig. 3. According to the NSJ theory, there are hole/electron sheet charges of large concentrations at the interface between GaN and AlGaN, the top AlGaN surface and the bottom GaN surface (Fig. 3(a)), which results in severe electric filed crowding at the corresponding p^+/2DEG and n^+/2DHG junctions shown in Fig. 3(c-d) and highlighted by the insets therein. On the other hand, the charges are uniformly distributed in the n and p-pillars of the LPSJ, therefore, the electric field crowding problem is significantly suppressed; e.g. the insets show >2x reduction in the peak electric field.

[1] T. Fujihira , *JJAP,* 36, 6254(1997). [2] L. Lorenz *et al. ISPSD*, (1999). [3] Z. Li *et al. IEEE TED*, 60, 3230 (2013). [4] H. Ishida *et al. IEEE IEDM,* (2008). [5] D. Jena *et al. APL 81, 4395* (2001). [6] J. Simon *et al. Science 327, 60* (2010). [7] J. Guo, *et al IEEE EDL*, 33,525(2012). [8] G. Li, *et al. IEEE EDL*, 34,852(2013). [9] J. Simon *et al. IEEE DRC (2008)*. [10] S. Li *et al. APL 101, 122103* (2012). [11] S. Rajan *et al*. *APL 88, 042103* (2006).

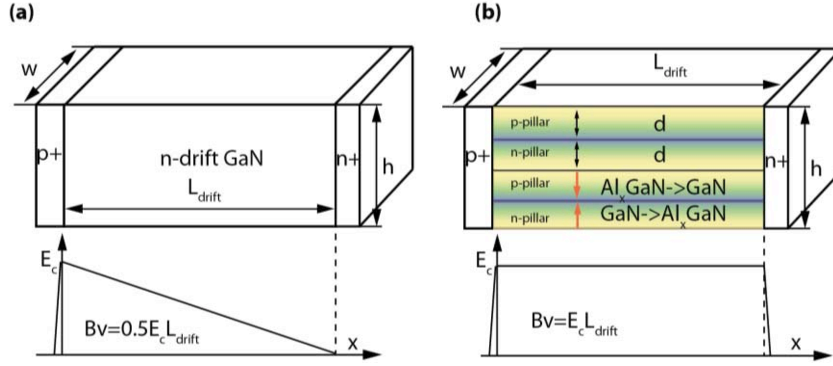

Fig.1 Conventional p-n diodes (a) and lateral polarization-doped super-junction (PolarSJ) diodes (b). The top figures show the device structures and dimensions and the bottom figures compare the electric field distribution. The flat field profile in LPSJ results from the balanced charge in the drift region thus a higher V_{br} for the same R_{on}.

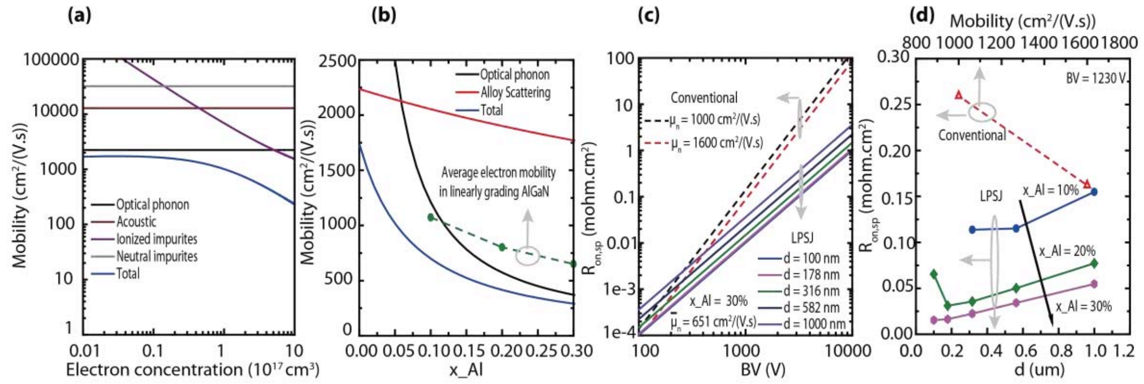

Fig.2 Calculated electron mobility in (a) Si-doped GaN with varying electron concentration and (b) polarization-doped AlGaN with varying Al composition; the average electron mobility in linearly graded Al_xGaN with $x_{Al} = 0 \rightarrow 10\%$, 20%, 30% is shown in green symbols (a polarization doping level of $2x10^{16}$ cm^{-3} is assumed). (c) Comparison of R_{on}-V_{br} between the impurity-doped conventional junction and the polarization-doped super junction with the pillars linearly graded from GaN to $Al_{0.3}GaN$. For BV > 300 V, the LPSJ offers a substantially lower $R_{on,sp}$ than the conventional p-n junctions. (d) Dependence of $R_{on,sp}$ on the pillar width d. Near 1200 V, ~10x lower $R_{on,sp}$ can be achieved in a LPSJ than the conventional junctions (red triangles). An optimal pillar width of ~200 nm is predicted for $Al_{x=0\rightarrow 20\%}GaN$ pillars.

$$R_{on,sp_L} = \frac{1}{q\mu N_D} \times \frac{L_{drift}}{wh'} \times A = \frac{1}{q\mu N_D} \times \frac{L_{drift}}{wh'} \times wL_{drift}$$

$$= \frac{1}{q\mu N_D} \times \frac{L_{drift}^2}{wh'}$$

$$h' = m(d - d_{dep}) \quad and \quad h = 2md$$

$$d_{dep} = \sqrt{\frac{2\varepsilon_s V_{bi}}{q}\left(\frac{1}{N_A} + \frac{1}{N_D}\right)}$$

$$N_A = N_D = \frac{\sigma_\pi}{d}$$

$$V_{bi} = \frac{K_B T}{q} In\left(\frac{N_A N_D}{n_i^2}\right)$$

$$BV = E_c L_{drift}$$

$$R_{on,sp_L} = \frac{BV^2}{q\sigma_\pi \bar{\mu} E_c^2} \times \frac{2d^2}{h(d - d_{dep})}$$

Table.1 Derivation of relationship between BV and $R_{on,sp}$ of LPSJ

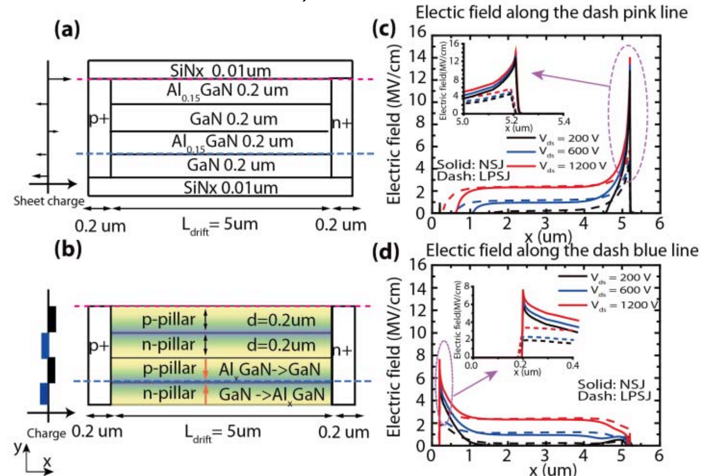

Fig.3 The drift region charge distribution along the vertical direction in a NSJ (a) and a LPSJ (b) with the same dimensions, and the simulated electric field distribution along the top surface marked by a pink dash line (c) and along a junction inside the device marked by a blue dash line (d). The insert shown in (c) and (d) indicate severe electric field crowding in NSJ while the peak electric field in LPSJ is at least 2x smaller.